Least-squares joint imaging of primaries and multiples

Morgan Brown, Stanford University*

SUMMARY

Multiple reflections, although usually treated as noise, often provide additional information about the corresponding primary reflections. I implement a least-squares inversion scheme to jointly image (by normal moveout) primaries and multiples. To achieve crosstalk suppression, I introduce a novel form of model regularization which exploits kinematic similarities between imaged primaries and multiples, and which also preserves the AVO response of the data. In tests on synthetic data, my approach exhibits good noise suppression and signal preservation characteristics. Real data tests highlight the need for careful data preprocessing. Future work points toward use of migration as the imaging operators, to exploit cases where multiples better illuminate some reflectors, and thus add considerable new information to the inversion.

INTRODUCTION

Multiple reflections have long been treated as noise in the seismic imaging process. In contrast to many other types of "noise", like surface waves, multiply reflected body waves may still penetrate deep into the earth, and thus have a potential to aid in imaging the prospect zone. I refer generically to *joint imaging with multiples* as any process which creates a "pseudo-primary" image from multiples by removing the propagation effects of body waves through arbitrary multiple layer (generator + free surface), and which then seeks to integrate the information provided by the primary and pseudo-primary images.

Reiter et al. (1991) present an early example of imaging multiples directly using a prestack Kirchhoff scheme. Yu and Schuster (2001) describe a cross-correlation method for imaging multiples. Berkhout and Verschuur (1994) and Guitton (2002) apply shot-profile migration for multiples. The aforementioned approaches produce separate-but-complementary primary and pseudo-primary images, yet they either do not attempt to, or employ simplistic methods to integrate the information contained in the two images. Youn and Zhou (2001) present a novel migration scheme which solves the two-way elastic wave equation and simultaneously images all primaries and multiples, although the computer memory requirements appear staggering by today's standards.

In this paper, I introduce a new methodology to jointly image primaries and multiples. My approach is driven by three primary motivations, in addition to the desire to correctly image the multiples:

1. **Data Consistency** - The primary and pseudo-primary images must both be consistent with the input data.
2. **Self-consistency** - The primary and pseudo-primary images must be consistent with one another, both kinematically and in terms of amplitudes.
3. **Noise Suppression** - In both the primary and pseudo-primary images, crosstalk must be suppressed.

To address all three requirements I adopt an approach similar to Nemeth et al. (1999), which used least-squares optimization to jointly image compressional and surface waves for improved wavefield separation. In my approach, data consistency is effected by minimization of a data residual; self-consistency and noise suppression by the use of regularization terms which penalize 1) differences between primary and pseudo-primary images, and 2) attributes which are not characteristic to true primaries or pseudo-primaries.

METHODOLOGY

NMO for Multiple Reflections

In a 1-D earth, multiple reflections can be treated as kinematically-equivalent primaries with the same source-receiver spacing but additional zero-offset traveltime τ^*, as illustrated in Figure 1. We can write an extension to the NMO equation which flattens multiples to the zero-offset traveltime of the reflector of interest.

$$t^2 = \sqrt{(\tau + j\tau^*)^2 + \frac{x^2}{V_{eff}^2}} \tag{1}$$

$j\tau^*$ is the two-way traveltime of a j^{th}-order multiple in the top layer. $V_{eff}(\tau)$ is the effective RMS velocity of the equivalent primary shown in the figure. For the simple case of constant velocity, v^*, in the multiple-generating layer,

$$V_{eff}(\tau) = \frac{\tau^* v^* + \tau V(\tau)}{\tau^* + \tau} \tag{2}$$

Thus, for the case of relatively flat reflectors, $v(z)$, and short offsets, equation (1) flattens water-bottom multiples of any order to the τ of interest, given a picked water bottom (τ^*).

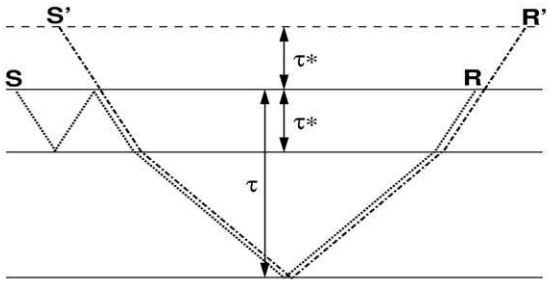

Figure 1: Schematic for NMO of multiples. Multiples can be treated as pseudo-primaries with the same source-receiver spacing, but with extra zero-offset traveltime τ^*, assuming that the velocity and time thickness of the multiple-generating layer are known.

AVO of Multiple Reflections

Even after application of the water-bottom reflection coefficient, the AVO signature of the pseudo-primary section created by equation (1) does not match that of the corresponding NMO-corrected primary section. Refer to Figure 2 and note that, under the assumptions of a constant-AVO water-bottom reflection and a free surface reflection coefficient of -1, the amplitude of the water-bottom multiple at offset $h_p + h_m$ is simply the amplitude of the primary at offset h_p, scaled by the negative water-bottom reflection coefficient. For the case of constant velocity, we can use trigonometry to derive h_m and h_p as a function of the zero offset traveltimes of the primary reflection and water bottom (τ and τ^*, respectively), and the source-receiver offset x. In constant velocity, the multiple and primary legs of the raypath are similar triangles:

$$\frac{\tau v}{h_p} = \frac{\tau^* v}{h_m}. \tag{3}$$

Also, for a first-order water-bottom multiple,

$$h_p + h_m = x.$$

These two independent equations can be solved and simplified to give expressions for h_p and h_m:

$$h_p = \frac{\tau}{\tau+\tau^*}x \qquad \text{and} \qquad h_m = \frac{\tau^*}{\tau+\tau^*}x. \tag{4}$$

The general form of the expression, for orders of multiple higher than one, is straightforward to derive.

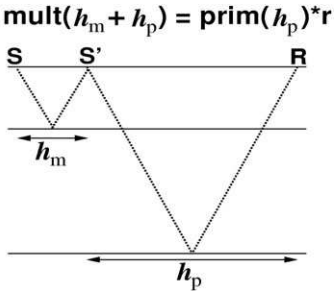

Figure 2: The AVO of water-bottom multiples with offset $h_p + h_m$ is a function of the AVO of the primary recorded at h_p.

Least-squares imaging of multiples

Applied to a common-midpoint gather, equation (1) produces an approximate unstacked zero-offset image of pseudo-primaries from water bottom multiple reflections. In this section, I introduce a least-squares scheme to compute self-consistent images of primaries and pseudo-primaries which are in turn consistent with the data. First I define some terms:

- $\mathbf{d}$ $\leftrightarrow$ One CMP gather.
- $\mathbf{m}_j$ $\leftrightarrow$ Prestack model vector for multiple order j. Produced by applying equation (1) to $\mathbf{d}$.
- $\mathbf{N}_j$ $\leftrightarrow$ *Adjoint* of NMO for multiple of order j (primaries: $j=0$). $\mathbf{N}_j^T$ applies equation (1) to $\mathbf{d}$.
- $\mathbf{R}_j$ $\leftrightarrow$ Given a single water-bottom reflection coefficient, r, this operator scales $\mathbf{m}_j$ by $1/r^j$ to make the amplitudes of all the $\mathbf{m}_j$ comparable.

We can now write the forward modeling operator for joint NMO of primaries and multiples of order 1 to p.

$$\left[\mathbf{N}_0 \;\; \mathbf{N}_1\mathbf{R}_1 \;\cdots\; \mathbf{N}_p\mathbf{R}_p\right] \begin{bmatrix} \mathbf{m}_0 \\ \mathbf{m}_1 \\ \vdots \\ \mathbf{m}_p \end{bmatrix} = \mathbf{Lm} \tag{5}$$

Equation (5) takes a vector of psuedo-primary panels, divides each element by the appropriate reflection coefficient, applies inverse (adjoint) NMO to each element, and then sums them together to create something that should resemble "data". We define the data residual as the difference between the input data and the forward-modeled data:

$$\mathbf{r}_d = \mathbf{d} - \mathbf{Lm} \tag{6}$$

Taken alone, the above least-squares system is underdetermined. Additional regularization terms, defined below, force the problem to be overdetermined.

Consistency of the Data and the Crosstalk Problem

Figure 3 illustrates the application (the adjoint) of equation (5) to a synthetic CMP gather. Imagine that the CMP gather consisted only of primaries and first- and second-order water-bottom multiples; the "NMO for Primaries" panel would contain flattened primaries (signal) and downward-curving first- and second-order multiples ["crosstalk" (see Claerbout (1992))]. Likewise, the "NMO for multiple 1" and "NMO for multiple 2" panels would contain flattened signal and curving crosstalk. If each of the three panels contained all signal and no crosstalk, then we 1) could perfectly reconstruct the data from the model by applying equation (5), and 2) would have a perfect estimate of the primaries.

Unfortunately, the crosstalk in all three model panels spoil this idealized situation. Crosstalk events map back to actual events in the data, so they are difficult to suppress in a least-squares minimization of the data residual [equation (6)]. Nemeth et al. (1999) shows that crosstalk relates directly to non-invertibility of the Hessian ($\mathbf{L}^T\mathbf{L}$), and that data-space or model-space regularization may partially solve the problem.

Regularization of the Least-Squares Problem

Visual inspection of Figure 3 motivates the two forms of model regularization utilized in this paper. Notice that the corresponding crosstalk events across the various panels all have different move-outs. In fact, the only kinematically-consistent events across all offsets are the flattened primary and pseudo-primaries. The first regularization operator seeks to penalize the difference between the $\mathbf{m}_i$, at fixed τ. To account for the dissimilarity of the AVO of primaries and multiples, this difference is taken at different offsets, as defined by equation (4). Written in the form of a model residual vector, this difference is:

$$\mathbf{r}_m^{[1]}(\tau,x,i) = m_i(\tau,h_p) - m_{i+1}(\tau,x). \tag{7}$$

The index i in equation (8) ranges from 0 to n_p-1, where n_p is the highest order multiple modeled in the inversion [equation (5)].

The second form of regularization is a difference operator along offset, which exploits the fact that all non-crosstalk events have residual curvature after NMO. Again, we can write this difference in the form of a model residual vector:

$$\mathbf{r}_m^{[2]}(\tau,x,i) = m_i(\tau,x) - m_i(\tau,x+\Delta x). \tag{8}$$

The second regularization is applied to all the $\mathbf{m}_i$. A similar approach is used by Prucha et al. (2001) to regularize prestack depth migration in the angle domain.

Combined Data and Model Residuals

To compute the optimal set of $\mathbf{m}_i$, a quadratic objective function, $Q(\mathbf{m})$, consisting of sum of the weighted L_2 norms of the data residual [equation (6)] and of the two model residuals [equations (7) and (8)], is minimized via a conjugate gradient scheme:

$$\min Q(\mathbf{m}) = \|\mathbf{r}_d\|^2 + \epsilon_m^2\|\mathbf{r}_m^{[1]}\|^2 + \epsilon_x^2\|\mathbf{r}_m^{[2]}\|^2 \tag{9}$$

The scalars ϵ_m and ϵ_x balance the relative importance of the two model residuals relative to the data residual.

RESULTS

Synthetic data tests

We begin with the results of testing the proposed algorithm on a single synthetic CMP gather, shown previously in Figure 3, which was generated using Haskell-Thompson elastic modeling. Figure 4 illustrates the application of the proposed algorithm to the synthetic data.

Comparing the raw data and estimated primary panels [$\mathbf{m}_0$ in equation (5)], notice that the algorithm nicely suppresses the strongest multiples at far offsets, although some residual multiple energy remains at the near offsets. The poorer performance at near offsets

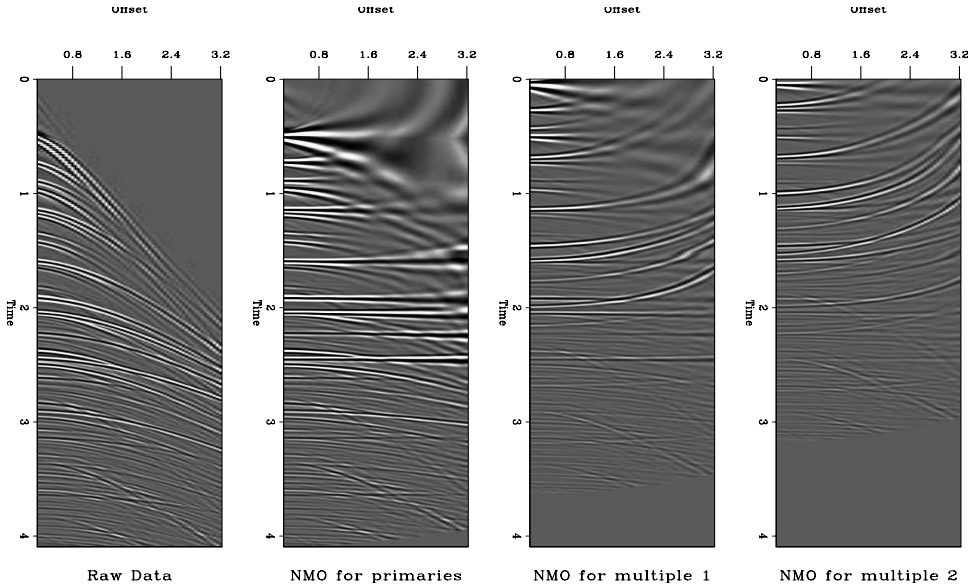

Figure 3: From left to right: Raw synthetic CMP gather; Conventional NMO applied to data; NMO for first-order water-bottom multiple; NMO for second-order water-bottom multiples.

is not unexpected; the first regularization operator [equation (7)] penalizes dissimilarity of events across orders of multiple, yet all orders of multiple align at near offsets. Moreover, the second regularization operator [equation (8)] penalizes residual curvature, yet all events in the section, both primaries and the residual multiples, are flat at near offsets.

The difference panel shows little residual primary energy, which illustrates the favorable signal preservation capability of my approach. The bulk of the residual primary energy exists at far offsets and small times, where NMO stretch makes the primaries nonflat, and hence, vulnerable to smoothing across offset by equation (8).

A Real Data Example

I test the proposed algorithm on a single CMP gather from the "Mobil AVO" dataset, provided by then-Mobil for use in the SEG 1995 multiples workshop. The synthetic CMP gather shown earlier is modeled after this real data. The results are shown in Figure 5. Relative to the results seen on the Haskell synthetic, they are mixed. The primary events are well-preserved, and the earliest water-bottom multiples are suppressed quite effectively, although the later reverberations are left almost untouched. Many factors likely contribute to the less-than-perfect results, though at this time, I believe that the weakness of the water bottom reflection and a lack of amplitude balancing are the primary factors. problems.

CONCLUSIONS AND FUTURE DIRECTIONS

I presented a new approach for the joint imaging of primary and multiple reflections. My approach goes further than the separate imaging of multiples and primaries, or the separation of multiples and primaries. It integrates information from the multiples and primaries in a least-squares inversion, via a new regularization term which exploits the kinematic similarity of primaries and pseudo-primaries, and the kinematic dissimilarity of crosstalk terms to obtain a noise-free image of the primaries.

In the long run, this project must use migration, rather than NMO, as the imaging operator, to overcome the limiting assumptions. In geologically complex areas, multiples often provide better angular coverage than primaries over a recorded cable length. Systematic integration of this extra information could prove revolutionary in regions of poor illumination.

In tests on synthetic and real data, the removal of crosstalk events at near offsets was incomplete. The problem will likely remain, even if the move to migration is made. The excellent ability of the SRME-class (Verschuur et al., 1992) algorithms to predict multiples at near offset should be investigated.

REFERENCES

Berkhout, A. J., and Verschuur, D. J., 1994, Multiple technology: Part 2, migration of multiple reflections: 64th Ann. Internat. Mtg, Soc. Expl. Geophys., Expanded Abstracts, 1497–1500.

Claerbout, J. F., 1992, Earth Soundings Analysis: Processing Versus Inversion: Blackwell Scientific Publications.

Guitton, A., 2002, Shot-profile migration of multiple reflections: SEP–**111**, 17–33.

Nemeth, T., Wu, C., and Schuster, G. T., 1999, Least-squares migration of incomplete reflection data: Geophysics, **64**, no. 1, 208–221.

Prucha, M. L., Clapp, R. G., and Biondi, B. L., 2001, Imaging under salt edges: A regularized least-squares inversion scheme: SEP–**108**, 91–104.

Reiter, E. C., Toksoz, M. N., Keho, T. H., and Purdy, G. M., 1991, Imaging with deep-water multiples: Geophysics, **56**, no. 07, 1081–1086.

Verschuur, D. J., Berkhout, A. J., and Wapenaar, C. P. A., 1992, Adaptive surface-related multiple elimination: Geophysics, **57**, no. 09, 1166–1177.

Youn, O., and Zhou, H.-W., 2001, Depth imaging with multiples: Geophysics, **66**, no. 1, 246–255.

Yu, J., and Schuster, G., 2001, Crosscorrelogram migration of IVSPWD data: 71st Ann. Internat. Mtg, Soc. Expl. Geophys., Expanded Abstracts, 456–459.

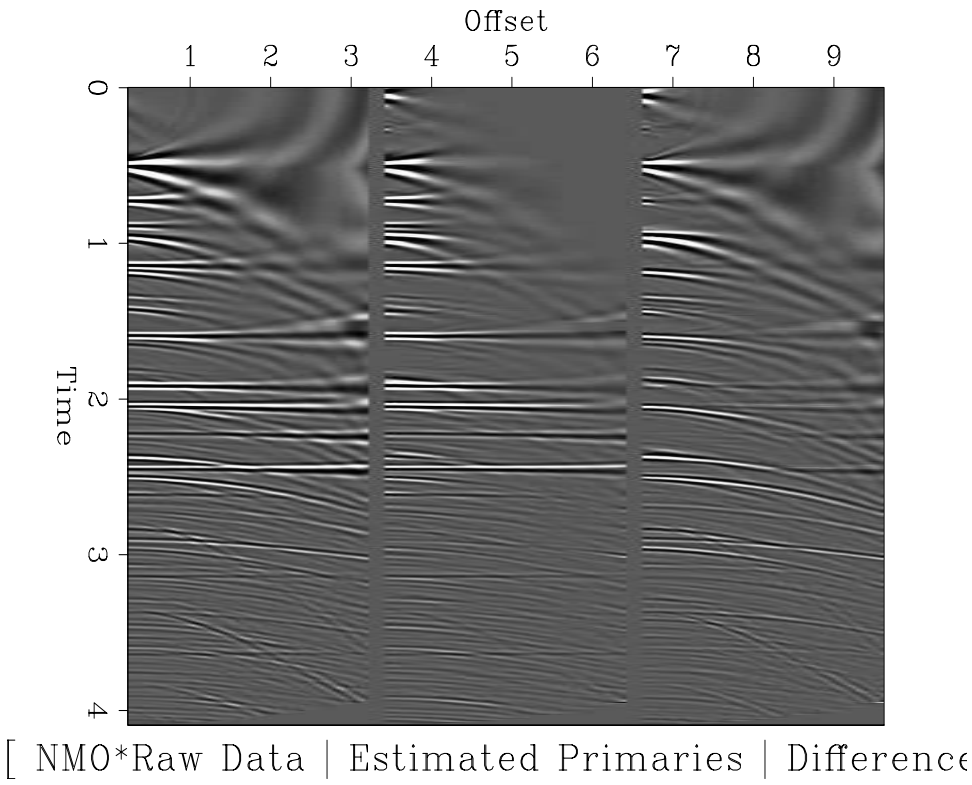

Figure 4: Test of equation (9) on synthetic CMP gather. Left to right: NMO'ed raw data; Estimated primary panel; difference panel.

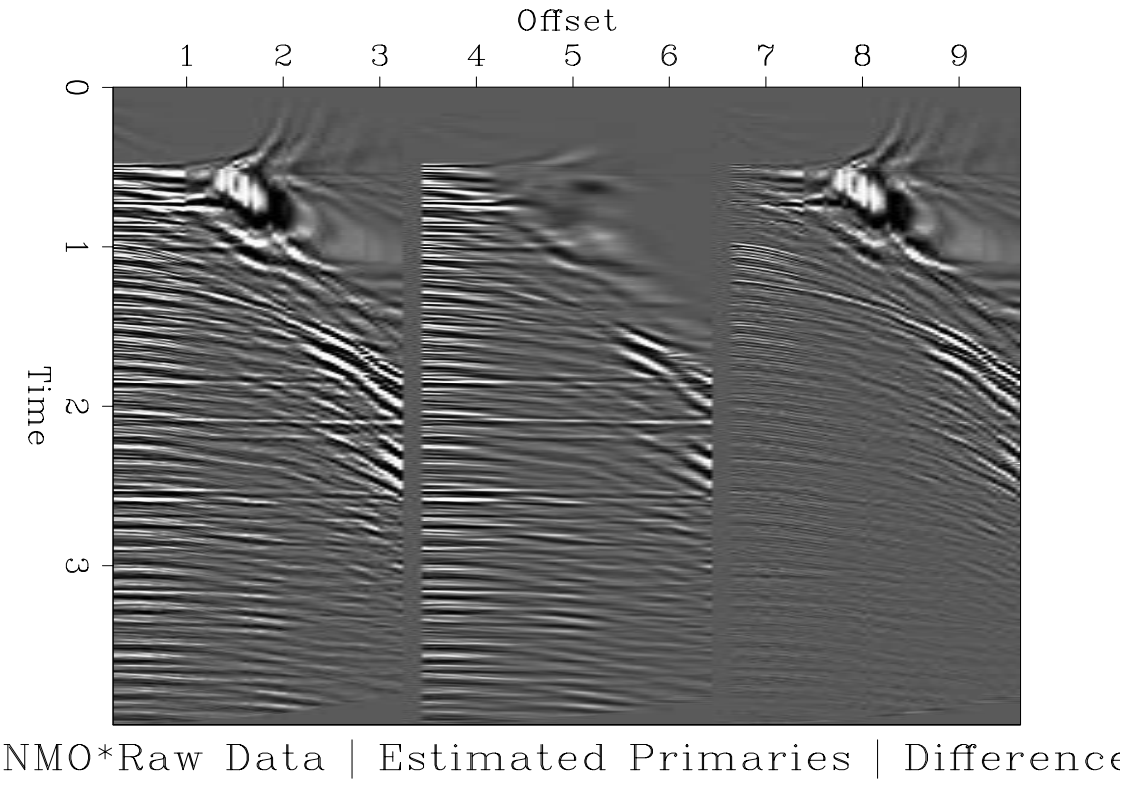

Figure 5: Application of equation (9) to real CMP gather. Left to right: NMO'ed raw data; Estimated primary panel; difference panel.